Transcriptional Differences between Normal and Glioma-Derived Glial Progenitor Cells Identify a Core Set of Dysregulated Genes

Romane M. Auvergne,[1,2,9,*] Fraser J. Sim,[1,2,5,9] Su Wang,[1,2] Devin Chandler-Militello,[1,2] Jaclyn Burch,[1,2] Yazan Al Fanek,[1,2] Danielle Davis,[1,2] Abdellatif Benraiss,[1,2] Kevin Walter,[1,3] Pragathi Achanta,[6] Mahlon Johnson,[4] Alfredo Quinones-Hinojosa,[6] Sridaran Natesan,[8] Heide L. Ford,[7] and Steven A. Goldman[1,2,*]

[1]Center for Translational Neuromedicine
[2]Department of Neurology
[3]Department of Neurosurgery
[4]Department of Pathology
University of Rochester Medical Center, Rochester, NY 14642, USA
[5]Department of Pharmacology, University of Buffalo, Buffalo, NY 14214, USA
[6]Department of Neurosurgery and Oncology, Johns Hopkins University School of Medicine, Baltimore, MD 21287, USA
[7]Department of Pharmacology, University of Colorado School of Medicine, Aurora, CO 80045, USA
[8]Sanofi-Aventis Pharmaceuticals, Cambridge, MA 02139, USA
[9]These authors contributed equally to this work
*Correspondence: romane_auvergne@urmc.rochester.edu (R.M.A.), steven_goldman@urmc.rochester.edu (S.A.G.)
http://dx.doi.org/10.1016/j.celrep.2013.04.035

SUMMARY

Glial progenitor cells (GPCs) are a potential source of malignant gliomas. We used A2B5-based sorting to extract tumorigenic GPCs from human gliomas spanning World Health Organization grades II–IV. Messenger RNA profiling identified a cohort of genes that distinguished A2B5[+] glioma tumor progenitor cells (TPCs) from A2B5[+] GPCs isolated from normal white matter. A core set of genes and pathways was substantially dysregulated in A2B5[+] TPCs, which included the transcription factor SIX1 and its principal cofactors, EYA1 and DACH2. Small hairpin RNAi silencing of SIX1 inhibited the expansion of glioma TPCs in vitro and in vivo, suggesting a critical and unrecognized role of the SIX1-EYA1-DACH2 system in glioma genesis or progression. By comparing the expression patterns of glioma TPCs with those of normal GPCs, we have identified a discrete set of pathways by which glial tumorigenesis may be better understood and more specifically targeted.

INTRODUCTION

Gliomas are the most common primary intracranial neoplasms in humans, accounting for 80% of all malignant brain tumors. Current treatment strategies, including surgery, radiotherapy, and chemotherapy, only modestly improve patient survival (Stupp et al., 2005). The limited efficacy of these approaches is a consequence of both the rapid invasion of brain tissue by glioma cells and the rapid appearance of both chemo- and radioresistant lineages within treated tumors.

Gliomas may arise from transformed somatic stem and progenitor cells. Indeed, cells derived from many types of primary CNS malignancies, including periventricular tumors (Sim et al., 2006), medulloblastomas, and gliomas (Hemmati et al., 2003; Ignatova et al., 2002), exhibit multipotentiality and self-renewal in vitro, suggesting their derivation from, or regeneration of, a stem cell phenotype. In glioma, a discrete cohort of CD133^{+} cells was first reported to be wholly responsible for the initiation of new gliomas in immunodeficient recipients (Bao et al., 2006; Singh et al., 2004). However, a number of recent studies have expanded this picture by revealing that CD133-negative glioma cells are also tumorigenic, whereas not all CD133^{+} cells are (Nishide et al., 2009). These observations suggest the coexistence of multiple tumor-initiating phenotypes in gliomas, most especially in high-grade (HG) tumors.

The antigenic heterogeneity of tumor-initiating cells in gliomas may in part reflect the variety of potential cell types of origin of glioma. Several studies have reported that in rodents, gliomas may arise from neural stem cells of the ventricular subependyma (Alcantara Llaguno et al., 2009; Jackson et al., 2006). Yet, although humans resemble rodents in harboring persistent subependymal neural progenitors (Pincus et al., 1998; Sanai et al., 2004), adult humans retain much larger populations of multipotential glial progenitor cells (GPCs) in the subcortical white matter (WM), in numbers that dwarf those of the adult subependyma. They can be distinguished from other brain phenotypes by their expression of gangliosides recognized by monoclonal antibody (mAb) A2B5 (Nunes et al., 2003), as well as by NG2/CSPG4 and platelet-derived growth factor-α receptor (PDGFαR) expression (Nishiyama et al., 2009; Sim et al., 2011). Interestingly, these prototypic GPC markers are overexpressed in glioma (Ogden et al., 2008; Shih and Holland, 2006). Furthermore, in rodents, parenchymal GPCs can form tumors that mimic the genomic and histological profiles of human oligodendroglioma (OLG) (Lindberg et al., 2009; Persson et al., 2010) and
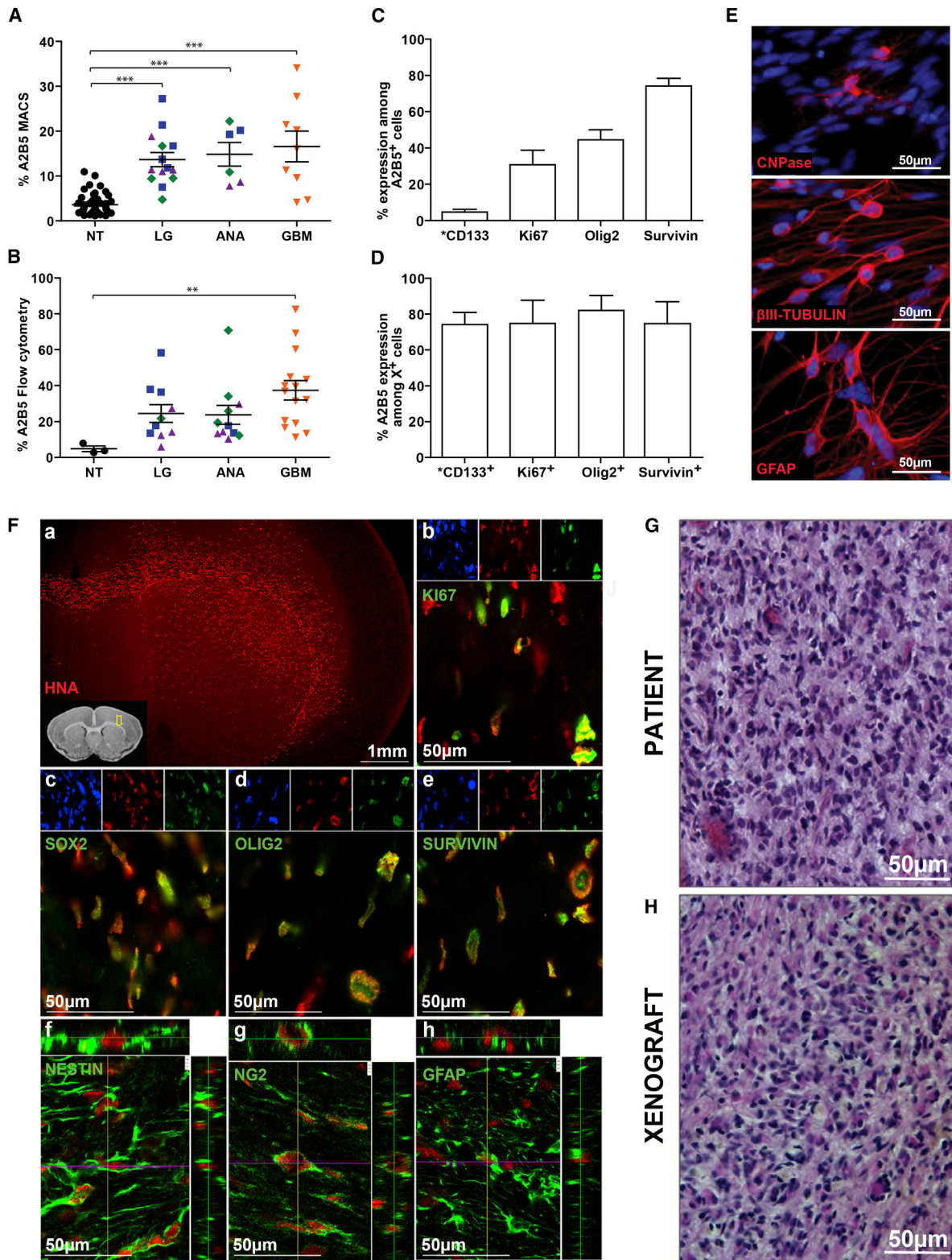
(legend on next page)

glioblastoma multiforme (GBM) (Assanah et al., 2006; Liu et al., 2011). Together, these data suggest that a proportion of human gliomas may arise from parenchymal GPCs. On that basis, we asked whether a subtractive genomics strategy comparing normal adult human GPCs with their identically sorted counterparts derived from adult gliomas would identify pathways specifically associated with human glial oncogenesis.

RESULTS

A2B5[+] Cells Are Abundant in Glioma and Manifest a Stem Cell Phenotype In Vitro

To assess the incidence of A2B5^{+} cells in adult gliomas, we used both magnetic activated cell sorting (MACS) and flow cytometry. By MACS, A2B5^{+} cells were significantly more abundant in gliomas (14.4% ± 1.3%, n = 29) than in noncancerous adult WM or cortex (3.6% ± 0.3%; n = 54; Figure 1A; Table S1). Flow cytometry, with less false-negatives than MACS, confirmed that A2B5^{+} cells were significantly more abundant in tumors (28.8% ± 3.2%; n = 35) than in nonneoplastic WM (2.9% ± 0.4%; n = 3; Figure 1B; Table S1). Although only a small fraction of these A2B5^{+} glioma cells coexpressed CD133 (4.6% ± 1.5%), almost half (45% ± 5.4%) coexpressed the oligodendroglial protein OLIG2 (Ligon et al., 2007), and most (74% ± 4.2%) also expressed the tumor marker Survivin (BIRC5). The A2B5^{+} glioma cells were highly mitotic: 31% ± 7.9% coexpressed Ki67 (Figures 1C and S1A). Of note, although CD133 was an uncommon phenotype in fresh tumors, most CD133^{+} cells (74% ± 6.7%) coexpressed A2B5, as did most OLIG2^{+}, Ki67^{+}, and SURVIVIN^{+} cells (≥75%; Figures 1D and S1A). To validate these cytometric data in situ, we identified glioma tumor progenitor cells (TPCs) in sections of GBMs by their nuclear coexpression of OLIG2 and Ki67 (Ligon et al., 2007). Whereas only a minority of OLIG2^{+} cells expressed Ki67 (34% ± 5.2%; n = 4), most Ki67^{+} cells expressed OLIG2 (78% ± 3.8%; Figures S1B and S1C). Similarly, whereas only 45% ± 5.4% of GBM-derived A2B5^{+} cells expressed OLIG2 in vitro (Figure 1C), 82% ± 8.1% of OLIG2^{+} cells were A2B5^{+} (Figures 1D and S1A). These data suggest that the A2B5 immunophenotype comprises a discrete fraction of glioma cells, which includes most CD133^{+} and OLIG2^{+}/Ki67^{+}/Survivin^{+} cells.

A2B5-Defined Tumor Progenitors Are Clonogenic, Self-Renewing, and Multipotential In Vitro

We next asked whether A2B5^{+} glioma cells are clonogenic in vitro. To that end, we isolated A2B5[+] and A2B5^{−} cells by fluo-

rescence-activated cell sorting (FACS) and raised each fraction in low-density suspension culture in serum-free media (Nunes et al., 2003). HG-glioma-derived A2B5^{+} cells robustly generated neurospheres with substantially greater efficiency than did their A2B5[−] homologs, as demonstrated by in vitro limiting dilution analysis (Figures S2A–S2D). To assess the lineage potential of A2B5-defined TPCs, we expanded isolated A2B5^{+} cells as neurospheres and plated them in 1% serum to promote their differentiation. Twelve days later, the resultant outgrowths were immunostained for the astrocytic marker glial fibrillary acidic protein (GFAP), the neuronal markers βIII-tubulin and MAP2, and the early oligodendroglial markers OLIG2 and 2′,3′-cyclic nucleotide 3′- phosphosdiesterase (CNP). Each of these phenotypes was present within single spheres (Figure 1E), suggesting that A2B5[+] TPCs, like normal GPCs (Nunes et al., 2003), retained multilineage competence in vitro.

Importantly, we found that A2B5 expression defined a preferentially expanding pool of glioma TPCs, and that its expression was sustained with propagation. We established stable lines from World Health Organization (WHO) stage IV gliomas (n = 5) and found that by the third passage, >98% of all cells were A2B5[+] (Figure S2E). These lines have now been passaged for over a year, and each has retained A2B5 expression, with concurrent expression of SOX2 (76% ± 16.8%) and Survivin (57% ± 7.5%; Figures S1A and S2F). Interestingly, whereas CD133 was only rarely expressed in freshly isolated glioma cells, most A2B5^{+} glioma cells developed CD133 expression with propagation (Figures S2G and S2H). Conversely, virtually all SOX2^{+}, Survivin^{+}, OLIG2^{+}, and Ki67^{+} cells in these cultures (>97% for each), as well as most CD133^{+} cells (88% ± 6.7%), coexpressed A2B5 (Figure S1A). In contrast to the sustained self-renewal competence of A2B5^{+} TPCs sorted from HG gliomas and GBMs, those derived from low-grade (LG) WHO II gliomas were only able to generate spheres at early passages. These cultures could not be maintained beyond 5 months, reflecting the limited self-renewal competence of LG glioma cells (Galli et al., 2004). These observations suggested that human GBM cells rapidly select for an A2B5 phenotype with repetitive passage in vitro, and that virtually all SOX2^{+} and CD133^{+} glial TPCs coexpress A2B5 immunoreactivity.

A2B5-Defined Tumor Progenitors Express Telomerase as a Function of Grade

To assess the basis for the differential self-renewal competence of LG- and HG-glioma-derived A2B5^{+} cells, we asked whether

Figure 1. In Vitro and In Vivo Characterization of Glioma-Derived A2B5[+] Cells

(A and B) A2B5-based MACS (A) and flow cytometry analysis (B) of freshly dissociated gliomas and nonneoplastic WM and cortex. Horizontal lines indicate the mean percentage of A2B5^{+} cells ± SEM. Triangles represent astrocytoma (AST); squares represent oligodendroglioma (OLG); diamonds indicate oligoastrocytoma (**p < 0.02, ***p < 0.001; Kruskal-Wallis test). NT, nontumor; ANA, anaplastic astrocytoma/oligoastrocytoma..

(C and D) Dual-flow cytometry (*) and immunocytochemical analysis of freshly isolated GBM cells stained for A2B5, CD133, Ki67, Olig2, and Survivin. Data are expressed as mean ± SEM.

(E) Immunostaining of GBM-derived A2B5^{+} cells cultured under differentiating conditions for CNPase, β3-tubulin, and GFAP markers (red). Nuclei were counterstained with DAPI (blue).

(F) Coronal sections through a mouse brain transplanted with GBM-derived A2B5^{+} human cells, stained with the human-specific antigen antibody (red, a–h) and (green) Ki67 (b), Sox2 (c), Nestin (f), Olig2 (d), NG2 (g), Survivin (e), and GFAP (h). Cells were counterstained with DAPI (blue).

(G and H) Hematoxylin and eosin (H&E)-stained sections of a patient's tumor (H) and its derived A2B5-sorted xenograft in an adult mouse (I).

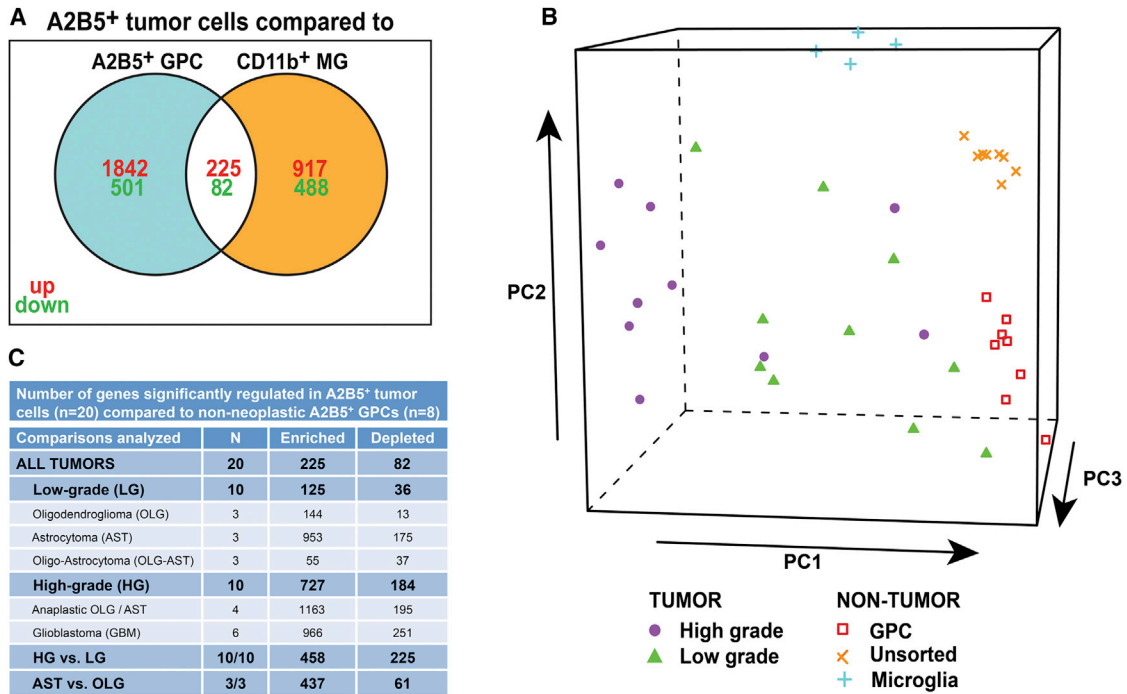See also Figures S1, S2, S3, and S4 and Tables S1 and S10.

A A2B5+ tumor cells compared to

C

Number of genes significantly regulated in A2B5+ tumor cells (n=20) compared to non-neoplastic A2B5+ GPCs (n=8)			
Comparisons analyzed	**N**	**Enriched**	**Depleted**
ALL TUMORS	20	225	82
Low-grade (LG)	10	125	36
Oligodendroglioma (OLG)	3	144	13
Astrocytoma (AST)	3	953	175
Oligo-Astrocytoma (OLG-AST)	3	55	37
High-grade (HG)	10	727	184
Anaplastic OLG / AST	4	1163	195
Glioblastoma (GBM)	6	966	251
HG vs. LG	10/10	458	225
AST vs. OLG	3/3	437	61

Figure 2. Differential Gene-Expression Profiles of A2B5+ Glioma Cells at All Stages of Gliomagenesis

(A and C) Venn diagram (A) and table (C) showing the number of genes up- or downregulated (>3 FC, 1% FDR) in A2B5+ TPCs versus both normal adult A2B5+ GPCs and CD11b+ microglial cells (MG) using Affymetrix gene expression microarrays.

(B) PCA. Green and purple, LG- and HG-derived A2B5+ cells; red, nontumor A2B5+ GPC; tangerine, unsorted normal cells; green cross, microglial cells.

See also Figures S5 and S6, and Tables S2, S3, S4, S5, S6, S7, S8, and S9.

these cells express telomerase enzymatic activity (Langford et al., 1995), and if so, at what stages of anaplastic progression they do so. Using the telomeric repeat amplification protocol assay (TRAP), we detected a significant degree of telomerase reverse transcriptase activity in five of six GBM-derived A2B5+ cell isolates. In contrast, no detectable telomerase activity was detected in either LG-derived A2B5+ cells or those derived from normal adult WM (Figure S3A). Together, these data suggest that telomerase induction is associated with malignant progression rather than with initial gliomagenesis, and provide a basis for the limited self-renewal competence of LG-glioma-derived A2B5+ TPCs.

A2B5-Sorted Cells Initiated New Gliomas in Immunodeficient Recipients upon Orthotopic Graft

To determine whether A2B5+ TPCs could independently initiate gliomas in naive hosts, we sorted freshly dissociated cells from six WHO stage II–IV gliomas using MACS or FACS into A2B5+ and A2B5− fractions, and then transplanted them over a range of 5,000–100,000 cells/graft into the corpus callosa of immunodeficient mice. The resultant xenografts were analyzed 6–15 weeks later (Figure S4A). Seventeen of 18 mice implanted with A2B5+ cells developed invasive gliomas by 6 weeks, whereas 13 of 16 mice transplanted with A2B5− cells from the same tumors did so. No significant differences were noted in the distribution, volume, or Ki67 index of tumors derived from MACS-sorted A2B5+ and A2B5− cells (Figures S4B–S4E).

Interestingly, the three mice that failed to develop tumors from A2B5− grafts were those given the lowest dose (5,000 cells), which was invariably tumorigenic when A2B5+ cells were used. Thus, both A2B5+ and A2B5− TPCs were tumorigenic upon xenograft, although in vivo limiting dilution analysis suggested preferential tumorigenesis by the A2B5+ fraction, as reported previously (Ogden et al., 2008; Tchoghandjian et al., 2010). The A2B5+ xenografts were both highly migratory (Figure 1Fa) and highly proliferative, with a Ki67 index of 27.1% ± 2% (n = 11; Figure 1Fb). Like the tumors from which they derived, the grafts expressed Survivin, SOX, nestin, OLIG2, NG2, and GFAP proteins (Figure 1F, c–h), and assumed the histological appearance of native GBMs (Figures 1G and 1H).

Expression Profiling Revealed an A2B5+ TPC Gene-Expression Signature

We next sought to identify the molecular concomitants to the transformation of A2B5+ TPCs using Affymetrix U133+2 microarrays. A2B5+ tumor cells derived from both LG (WHO grade II, n = 10) and HG (WHO grade III-IV, n = 10) gliomas (Table S2) were compared with their A2B5+ counterparts derived from normal adult WM (n = 4) and cortex (n = 4). In addition, because microglia may be recognized by both A2B5 and NG2 antibodies (Pouly et al., 1999), we also profiled CD11b+ human microglia sorted from adult epileptic resections (n = 4) so as to establish a filter that would exclude microglial transcripts from our TPC gene sets (Figure 2A). Principal-component analysis (PCA) confirmed

that A2B5+ cells isolated from both LG and HG gliomas showed overall expression profiles that were readily distinguished from those of normal adult GPCs, unsorted tumor cells, and microglia (Figure 2B).

To define those genes whose expression distinguishes A2B5+ TPCs (n = 20) from nonneoplastic GPCs (n = 8), we performed differential gene-expression analysis using relatively stringent cutoffs (>3-fold change [FC], 1% false discovery rate [FDR]) and identified a total of 355 dysregulated genes (226 up, 113 down; Figure 2C; Tables S3 and S4). To further identify grade-associated changes in A2B5 expression signature, we separately compared the profiles of A2B5+ cells derived from LG and HG gliomas with those of A2B5+ GPCs, as well as with one another, so as to identify genes associated with anaplastic progression (Figure 2C; Tables S3 and S4). We then separately compared the expression patterns of OLG and astrocytoma (AST) A2B5+ cells (WHO grade II) with one another, as well as with normal A2B5+ GPCs (Figures 2C and S5; Tables S3 and S4), so as to distinguish between gene sets associated with early stages of glioma progression and those involved in fate determination.

Among the genes dysregulated in glioma-derived TPCs, we focused initially on those genes with the highest expression ratios in all A2B5+ tumor cells relative to normal GPCs (Figure 3A and Table 1). We found only eight genes that were ≥10-fold overexpressed in TPCs at all levels of anaplastic progression (Figure 3A), among which CD24, GAP43, MMP3, and IGFBP3 have been previously associated with invasive glioma. In addition, this analysis revealed a set of genes that were not previously known to be involved in gliomagenesis, including SIX1, EYA1, SATB2, and CSRP2. Interestingly, the transcription factor SIX1 and its coactivating binding partner, EYA1, have been shown to participate in the oncogenesis of human mammary carcinoma cells (Christensen et al., 2008; Pandey et al., 2010). Similarly, SATB2 and CSRP2 have been related to disease progression in carcinoma (Midorikawa et al., 2002; Patani et al., 2009). Several other oncogenes were also highly overexpressed, albeit by <10-fold; these included epidermal growth factor receptor (EGFR), MYC, and the inhibitor of differentiation genes ID1 and ID4 (Table S3). In addition, a number of genes were downregulated by A2B5+ TPCs at all stages of progression (n = 113; Table S4), six by >10-fold (Figure 3B). Several of these genes have been described as tumor suppressors, including MTUS1 (Di Benedetto et al., 2006) and SPOCK3 (Earl et al., 2006). Quantitative PCR (qPCR) confirmed the dysregulation of selected genes (Figure 3C; Table S9). By defining those gene sets that were dysregulated in A2B5+ TPCs relative to their normal adult homologs in both LG and HG gliomas, we identified a discrete cohort of genes associated with both the initial appearance and the anaplastic progression of glioma.

A2B5+ Glioma Cells Overexpressed Transforming Growth Factor β, Bone Morphogenetic Protein, and Wnt Pathway Components

To identify which pathways were the most selectively dysregulated in A2B5+ glioma TPCs relative to their normal homologs, we applied a set of functional (Gene Ontology [GO] and Kyoto Encyclopedia of Genes and Genomes [KEGG]) and pathway (Molecular Signatures Database [mSigDB] and ingenuity pathway analysis [IPA]) databases to the list of differentially expressed genes (by >3 FC, 1% FDR). Our analysis revealed a strong enrichment for genes associated with cancer, cell proliferation, cell migration, and motility in both LG- and HG-derived A2B5+ cells, suggesting that neoplastic A2B5+ cells have greater proliferative and migration competence than their homologs derived from normal brain (Figure S6B; Table S5). Among specific gene sets that were overrepresented in A2B5+ TPCs, GO revealed a significant enrichment of genes involved in both Wnt/β-catenin and bone morphogenetic protein (BMP) signaling, whereas KEGG analysis highlighted the transforming growth factor β (TGF-β) signaling pathway as being the most significantly overrepresented (Table S5). IPA confirmed the predominant association of both TGF-β pathway and Wnt/β-catenin-associated genes with glioma TPCs (Figures 3D and 3E; Tables S5 and S8). Similarly, gene set enrichment analysis (GSEA) revealed an overrepresentation in A2B5+ TPCs of MYC target genes (Table S5).

A2B5+ Cells Derived from LG Glioma Expressed a Proneural Signature

Having defined the genes that were differentially expressed in A2B5+ TPCs at all stages of progression, we next focused on the genes that accompanied early tumorigenesis. We compared the expression profiles of LG-derived A2B5+ cells with those of their normal A2B5+ homologs and identified a set of 161 differentially expressed genes (Figure 2C). Among these were a small cohort of >10-fold overexpressed genes, including tumor-associated transcripts such as CD24, EYA1, and SIX1, as well as neurogenesis-associated genes such as NEUROD1, INA, SATB2, and ELAVL2, all of which are suggestive of a proneural (PN) phenotype (Figure 4A; Table S6). In contrast, among those genes that were significantly downregulated in LG A2B5+ cells, we identified several tumor suppressors not previously associated with gliomagenesis, including MTUS1, GPNMB, and RGN, as well as several markers of mature oligodendrocytes, including MOBP, OPALIN, and ASPA (Figure 4B; Table S6). In addition, GO- and KEGG-based analyses revealed a significant upregulation of genes associated with the BMP and TGF-β signaling pathways, and mSigDB similarly revealed enrichment of MYC-induced and associated genes (Table S6). IPA revealed an overrepresentation of genes related to Wnt/β-catenin and AMP-activated protein kinase signaling pathways (Tables S6 and S8).

LG and HG A2B5+ TPCs Exhibit Expression Profiles of Known Molecular Subclasses of GBM

We next used GSEA to evaluate the relationships between the A2B5+ TPC signature and previously established tissue-based data sets describing the major molecular subclasses of human GBM, and GBM-derived CD133+ TPC gene sets (Figure 5A). We first compared the profiles of neoplastic A2B5+ cells with those of unsorted nontumor cells, and observed a preferential enrichment of the PN signature in LG tumors, whereas HG-derived A2B5+ TPCs were enriched for gene sets that typify the epithelial-mesenchymal transition (EMT), as well as the proliferative (PROLIF) and classical (CL) subtypes of GBM (Phillips et al., 2006; Verhaak et al., 2010; Figures 5C, S7, and S8A–S8C). As such, LG A2B5+ TPCs were enriched in gene sets
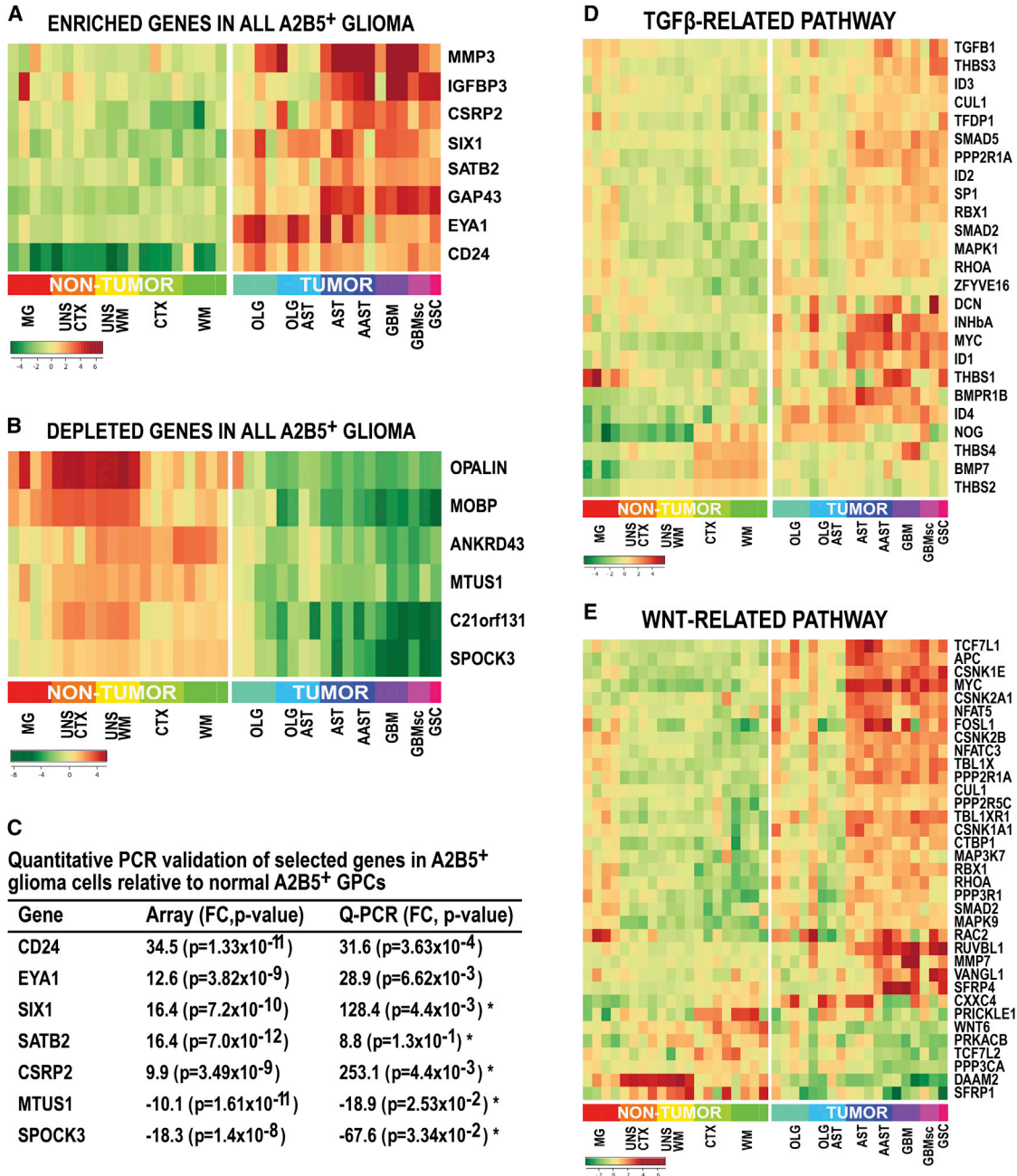
Figure 3. Specific Genes and Pathways Dysregulated in A2B5[+] Glioma Cells at All Stages of Gliomagenesis

(A and B) Heatmap representation of the top upregulated (A) and downregulated (B) genes (>10 FC) in A2B5^{+} TPCs, as assessed by microarray analysis and compared with normal A2B5^{+} GPCs derived from adult human WM, cortex (CTX), or CD11b^{+} microglia (MG).

(C) Real-time PCR validation of selected genes deregulated in A2B5^{+} TPCs relative to normal A2B5^{+} GPCs. Real-time PCR was performed using a 96-gene TaqMan low-density array (TLDA) or individual prevalidated Taqman assays (as indicated by *). Gene expression was normalized to glyceraldehyde 3-phosphate dehydrogenase (GADPH).

(D and E) Heatmap representation of GO- and KEGG-based pathways analysis of the TGF-β (D) and Wnt (E) pathways in A2B5^{+} TPCs relative to their non-neoplastic counterparts isolated from the adult human WM and CX, and CD11b^{+} MG. MG: microglia; UNS: unsorted cells; CTX: A2B5^{+} cells from normal cortex; WM: A2B5^{+} cells from normal white matter; AST: astrocytoma; AAST: anaplastic astrocytoma; GBM sc: small cell GBM; GSC: gliosarcoma.

See also Table S9.

associated with relatively prolonged patient survival, whereas the outcomes associated with the gene sets of HG A2B5$^+$ TPCs are less favorable (Freije et al., 2004). Importantly, both LG- and HG-derived A2B5$^+$ cells exhibited a significant enrichment of the CD133-UP signature, suggesting significant molecular homology between these tumor-initiating phenotypes (Figure 5C).

Interestingly, glioma-derived A2B5$^+$ cells also exhibited enrichment of the PN signature relative to their A2B5$^-$ counterparts, especially in LG tumors (Figures 5D and S8C). In contrast, the PN signature was depleted in neoplastic A2B5$^+$ cells relative to nonneoplastic GPCs, whereas MES/EMT-related gene sets were relatively enriched (Figures 5E, S7, and S8B). Together, these results indicate that LG- and HG-glioma-derived A2B5$^+$ cells respectively share features of PN and MES subclass GBMs, as well as GBM-derived CD133$^+$ TPCs, and that both may be distinguished from nonneoplastic GPCs by their selective overrepresentation of MES/EMT-related genes, which becomes more pronounced with anaplastic progression.

Anaplastic Progression of A2B5$^+$ TPCs Reflected an EMT

To more precisely define the grade-associated evolution in gene expression by A2B5$^+$ TPCs, we next compared the expression profiles of A2B5$^+$ cells derived from HG versus LG gliomas (>3 FC, 1% FDR), and identified a total of 683 dysregulated genes (Figure 2C; Table S7). Among these, 17 were overexpressed by >10-fold in HG-derived A2B5$^+$ cells; not surprisingly, these transcripts were related to transformation, invasion, angiogenesis, and a mesenchymal differentiation (Figure 4C). GSEA confirmed that many of these progression-associated genes were associated with the mesenchymal phenotype and EMT (Figure S7B; Table S7).

Among those genes that were downregulated in HG-derived A2B5$^+$ TPCs relative to their LG counterparts (n = 225; Figure 4D; Table S7), we identified the tumor suppressors SSTR1 (Patel, 1999) and SPOCK3 (Earl et al., 2006), the SIX1 repressor DACH2 (Christensen et al., 2008), and SHISA2, a regulator of the Wnt-β/catenin and fibroblast growth factor (FGF) signaling pathways (Hedge and Mason, 2008). KEGG-based functional analysis and IPA confirmed the relative dysregulation in HG A2B5$^+$ TPCs of Wnt/β-catenin signaling and IGF1-, p53-, Notch-, PI3/AKT-, and JAK-STAT-dependent pathways (Table S7). GSEA also demonstrated the differential overrepresentation of genes involved in cell motility, the TGF-β signaling pathway, and MYC target genes (Table S7). Together, these data indicate that the anaplastic progression of the A2B5$^+$ phenotype is associated with dysregulated gene expression within the Wnt/β-catenin and TGF-β pathways concurrently with an EMT, which is itself attended by both the increased expression of genes associated with motility and parenchymal invasion, and the downregulation of a discrete set of known tumor suppressors.

LG- and HG-Derived A2B5$^+$ Cells Share Common Gene-Expression Patterns with Human Embryonic Stem Cells and GPCs

To further explore the differentiated state of A2B5$^+$ glioma cells, we used GSEA to compare the gene-expression patterns of A2B5$^+$ TPCs with those of human embryonic stem cells (hESCs) and CD140a$^+$ (PDGFRα) GPCs, using published data sets (Figures 5B and 5F–5H). Interestingly, the hESC signature was enriched in both LG- and HG-derived A2B5$^+$ cells (Figures 5F–5H). In addition, when compared with unsorted nontumor brain cells as well as A2B5$^-$ glioma cells, both LG- and HG-derived A2B5$^+$ cells were strongly enriched for the CD140a$^+$ signature (Figures 5F and 5G). Accordingly, both microarray and qPCR analysis of marker genes revealed the selective enrichment in A2B5$^+$ TPCs of both GPC and NSC marker genes (Figures S9A–S9J). Interestingly, glioma-derived A2B5$^+$ cells could be readily distinguished from their nontumor homologs by the expression of the stem and mesenchymal marker CD44 (Figures S9D, S9E, and S9H), reflecting the selective expression by A2B5$^+$ glioma TPCs of the MES signature relative to normal, nonneoplastic GPCs.

SIX1 Inhibition Prevented the Growth, Proliferation, and Survival of GBM-Derived TPCs

The homeobox transcription factor SIX1 and its cofactor EYA1 were among the highest differentially expressed tumor transcripts in A2B5$^+$ TPCs relative to their nonneoplastic homologs (Figure 3C; Table 1; Table S9). qPCR confirmed that SIX1 messenger RNA (mRNA) was highly overexpressed by A2B5$^+$ cells isolated from both LG (231 ± 128 FC, n = 4; p < 0.001) and HG (76 ± 25 FC, n = 8; p < 0.001) gliomas relative to their nontumor A2B5$^+$ counterparts (n = 4), as well as in GBM-derived TPC lines (88 ± 51 FC, n = 5; p = 0.016; Figures 3C and S10A). Western immunoblots similarly revealed the high-level expression of SIX1 protein by primary gliomas and glioma cell lines, and its absence from the adult human brain (Figure S10B).

The robust overexpression of SIX1 in A2B5-defined TPCs, paired with its essential absence from the normal adult brain, prompted us to examine its contribution to gliomagenesis. To determine whether glioma TPCs were dependent on SIX1 protein-dependent signaling, we first tested the effects of lentiviral-induced knockdown (KD) of SIX1 (Figures S10C and S10D) on the growth of glioma TPCs in vitro. Lentiviral small hairpin RNAi (shRNAi) silencing of SIX1 (SIX1 KD) significantly reduced the number of GBM-derived TPCs relative to both scrambled (SCR) shRNAi-transduced and nontransduced control (CT) cells, 6 days posttransduction (p = 0.0005; Figures 6A and 6B). On that basis, we next investigated the effects of SIX1 KD on cell proliferation, cell-cycle progression, and cell survival. We found that SIX1 KD significantly reduced the mitotic fraction of bromodeoxyuridine (BrdU)-incorporating TPCs (24.3% ± 4.5%) relative to both SCR (32% ± 3.8%) and CT cells (36.3% ± 3.4%; p = 0.006; Figure 6C). We next addressed the role of SIX1 in cell-cycle progression by analyzing 5-ethynyl-2′-deoxyuridine (EdU) incorporation in association with propidium iodide staining. TPCs subjected to SIX1 KD manifested fewer cells in S phase (5.2% ± 1.1%) relative to SCR (8.8% ± 1.5%) and CT cells (9% ± 1.2%; p = 0.018; Figure 6D). We next asked whether SIX1 suppression might be associated with increased cell death, and found that SIX1 KD TPCs exhibited a significantly increased incidence of Annexin V-defined apoptotic death (33.9% ± 7.8%) compared with both SCR (24.7% ± 8.9%) and

Table 1. Significantly Dysregulated Genes in Glioma-Derived A2B5⁺ Cells Relative to Normal A2B5⁺ GPCs

Gene Symbol	Description	Fold Change	q Value
Transcription Factors			
SIX1	SIX homeobox 1	16.41	7.23×10^{-10}
SATB2	SATB homeobox 2	10.41	7.03×10^{-12}
FOXD1	forkhead box D1	8.27	1.41×10^{-8}
LOC100287917	hypothetical protein LOC100287917	8.22	6.57×10^{-7}
MYC	v-myc/c-myc	8.05	1.47×10^{-8}
SMARCA2	SWI/SNF-related, matrix-associated, actin-dependent regulator of chromatin	−6.40	9.13×10^{-9}
ST18	suppression of tumorigenicity 18 (breast carcinoma; zinc finger protein)	−3.06	6.32×10^{-3}
Ligands			
IL33	interleukin 33	6.91	6.71×10^{-6}
TNC	tenascin C	6.24	3.28×10^{-5}
INHbA	activin beta A	5.98	2.38×10^{-6}
STC2	stanniocalcin 2	5.97	7.82×10^{-9}
MIF	macrophage migration inhibitory factor (glycosylation-inhibiting factor)	5.68	2.39×10^{-8}
GREM1	Gremlin	−6.26	1.83×10^{-4}
GPNMB	glycoprotein (transmembrane) nmb	−6.00	2.23×10^{-7}
Receptors			
EGFR	epidermal growth factor receptor	9.04	3.86×10^{-7}
IL13RA2	interleukin 13 receptor, alpha 2	8.04	4.38×10^{-4}
CNR1	cannabinoid receptor 1 (brain)	5.21	2.66×10^{-7}
F2R	coagulation factor II (thrombin) receptor	4.59	2.84×10^{-7}
ADRA2A	adrenergic, alpha-2A-, receptor	3.97	2.02×10^{-4}
GPR37	G-protein-coupled receptor 37 (endothelin receptor type B-like)	−7.87	1.43×10^{-5}
TEK	TIE2	−6.28	6.31×10^{-6}
GRM3	glutamate receptor, metabotropic 3	−5.63	9.65×10^{-7}
LRP2	low-density lipoprotein-related protein 2	−5.48	1.21×10^{-4}
P2RY12	purinergic receptor P2Y	−3.80	4.50×10^{-3}
Other			
CD24	CD24 antigen (small cell lung carcinoma cluster 4 antigen)	34.53	1.33×10^{-11}
LOC100288551	hypothetical protein LOC100288551	19.31	6.17×10^{-11}
GAP43	growth-associated protein 43	15.00	8.99×10^{-10}
IGFBP3	insulin-like growth factor binding protein 3	11.77	2.41×10^{-5}
CSRP2	cysteine- and glycine-rich protein 2	9.91	3.49×10^{-9}
ANKRD43	ankyrin repeat domain 43	−20.75	1.29×10^{-10}
C21orf131	chromosome 21 open reading frame 131	−16.10	5.39×10^{-9}
MOBP	myelin-associated oligodendrocyte basic protein	−14.74	3.29×10^{-10}
OPALIN	oligodendrocytic myelin paranodal and inner loop protein	−11.98	2.81×10^{-9}
MTUS1	microtubule-associated tumor suppressor 1	−10.08	1.61×10^{-11}
Enzymes/Catalytic			
MMP3	matrix metalloproteinase 3 (stromelysin 1, progelatinase)	19.75	1.12×10^{-6}
EYA1	eyes absent homolog 1 (*Drosophila*)	12.67	3.82×10^{-9}
MGST1	microsomal glutathione S-transferase 1	9.48	4.83×10^{-7}
METT 7B	methyltransferase-like 7B	9.09	6.89×10^{-7}
EGFR	epidermal growth factor receptor	9.04	3.86×10^{-7}
ENPP2	ectonucleotide pyrophosphatase/phosphodiesterase 2 (autotaxin)	−9.02	2.07×10^{-8}
C5orf4	chromosome 5 open reading frame 4	−8.39	2.14×10^{-7}
PDK4	pyruvate dehydrogenase kinase, isozyme 4	−7.97	4.49×10^{-8}
ACACB	acetyl-coenzyme A carboxylase beta	−6.99	1.75×10^{-7}

Table 1. *Continued*

Gene Symbol	Description	Fold Change	q Value
GATM	glycine amidinotransferase (L-arginine:glycine amidinotransferase)	−6.57	5.44×10^{-7}
ECM/Cell Adhesion			
MMP3	matrix metalloproteinase 3 (stromelysin 1, progelatinase)	19.75	1.12×10^{-6}
LAMB1	laminin, beta 1	8.24	2.32×10^{-4}
TNC	tenascin C	6.24	3.28×10^{-5}
CCDC80	coiled-coil domain containing 80	5.67	1.35×10^{-7}
SPOCK3	sparc/osteonectin, cwcv, and kazal-like domains proteoglycan (testican) 3	−18.27	1.42×10^{-8}

Significantly dysregulated genes (>3 FC, 5% FDR) were annotated into functionally relevant categories. The top five from each category are shown in the table.

CT cells (20.3% ± 7.2%; p = 0.004; all comparisons by repeated-measures ANOVA; Figure 6E).

On the basis of these in vitro data, we examined the effects of SIX1 inhibition on the tumorigenic competence of A2B5$^+$ TPCs in vivo. TPC lines established from A2B5$^+$ cells derived from an anaplastic OLG and a GBM were transplanted into the brains of immunodeficient mice (6–8 × 10^4 cells/animal, n = 3 animals/group) 6 days after lentiviral transduction. SIX1 silencing inhibited the tumorigenicity of glioma TPCs, as demonstrated by a significant decrease in the number of hNA$^+$ cells at 6 weeks post-transplantation relative to SCR and CT cells (p = 0.01; Figures 6F and S10E). These observations indicate that SIX1 KD potently inhibits the growth, proliferation, and survival of A2B5-defined glioma TPCs both in vitro and in vivo, and suggest that SIX1 plays a critical role in the initiation and/or the proliferative expansion of malignant glioma.

DISCUSSION

In this study, we identified a core set of genes and pathways that are dysregulated throughout the anaplastic progression of glioma. We did so by comparing the gene-expression patterns of A2B5-sorted GPCs derived from the normal adult human brain with the expression patterns of their presumed homologs derived from gliomas at various stages of progression ranging from WHO II LG gliomas to grade IV GBM. We first validated both the robust self-renewal competence of A2B5$^+$ glioma TPCs and their diffuse invasion and efficient gliomagenesis when transplanted to immunodeficient hosts. We next assessed those genes and pathways that were differentially expressed by A2B5$^+$ TPCs relative to their normal homologs, and identified tumor-specific A2B5 transcript signatures as a function of both tumor stage and phenotype. Both LG- and HG-glioma-derived A2B5 signatures shared salient features of the transcription patterns of known GBM subtypes, GBM-derived CD133$^+$ TPCs, and hESCs. In particular, we identified the TGF-β and Wnt/β-catenin signaling pathways, as well as MYC, as being potently dysregulated in neoplastic A2B5$^+$ cells at every stage of tumor progression. These observations are in line with previous reports (Ikushima et al., 2009; Pulvirenti et al., 2011; Wang et al., 2008) and suggest that TGF-β, Wnt/β-catenin, and MYC signals all contribute to the initial transformation of GPCs, as well as to the subsequent maintenance and progression of malignant phenotype. Since both the TGF-β and Wnt/β-catenin pathways have been associated with the turnover of

normal neural stem cells and GPCs (Feigenson et al., 2009; Mishra et al., 2005), our identification of their tumor-progenitor-selective components may provide an especially compelling set of therapeutic targets.

This comparison revealed a core set of genes that were dysregulated during both the early and late stages of tumor progression. These transcripts included the selectin ligand CD24, the SIX1 homeodomain transcription factor and its binding partner EYA1, the dedifferentiation-associated gene SATB2, and the growth- and invasion-associated transcripts MMP3, IGFBP3, CSRP2, and GAP43. By virtue of their marked differential overexpression by TPCs at both early and late stages of glioma progression, these genes appear to comprise a promising set of targets for therapeutic intervention. To define which gene sets were preferentially associated with anaplastic progression and invasiveness, we also compared the expression patterns of A2B5$^+$ TPCs derived from HG tumors with those derived from lower-grade ASTs and OLGs. We found that with anaplastic progression, the A2B5$^+$ TPCs upregulated genes associated with the acquisition of mesenchymal phenotype, confirming prior studies using resected glioma tissues (Phillips et al., 2006; Verhaak et al., 2010). Importantly, the enrichment of EMT-associated genes, with a concurrent enrichment of genes involved in motility, suggests that the A2B5-defined pool includes those cells that are most associated with both malignant progression and parenchymal invasion.

Our analysis also identified a discrete set of genes that were highly differentially overexpressed during the initial and late stages of glioma progression, and thus constitute an especially attractive favorable set of therapeutic targets. These include the glycoprotein CD24, a glycophosphatidylinositol-anchored protein that has been associated with invasiveness and progression in a variety of solid tumors (Baumann et al., 2005). Our data are in accord with previous reports showing that CD24 protein is overexpressed in both LG and malignant gliomas, and is associated with poor prognosis and increased invasiveness (Deng et al., 2012; Senner et al., 1999).

We also identified the transcription factor SIX1 (*Sine oculis*) as the second-highest differentially expressed transcript by A2B5$^+$ TPCs derived from both LG and HG gliomas. Interestingly, SIX1 overexpression has been described in a number of solid tumors, including gliomas, and has been correlated with worse clinical prognosis (Micalizzi et al., 2009), whereas its misexpression can result in the transformation of human mammary
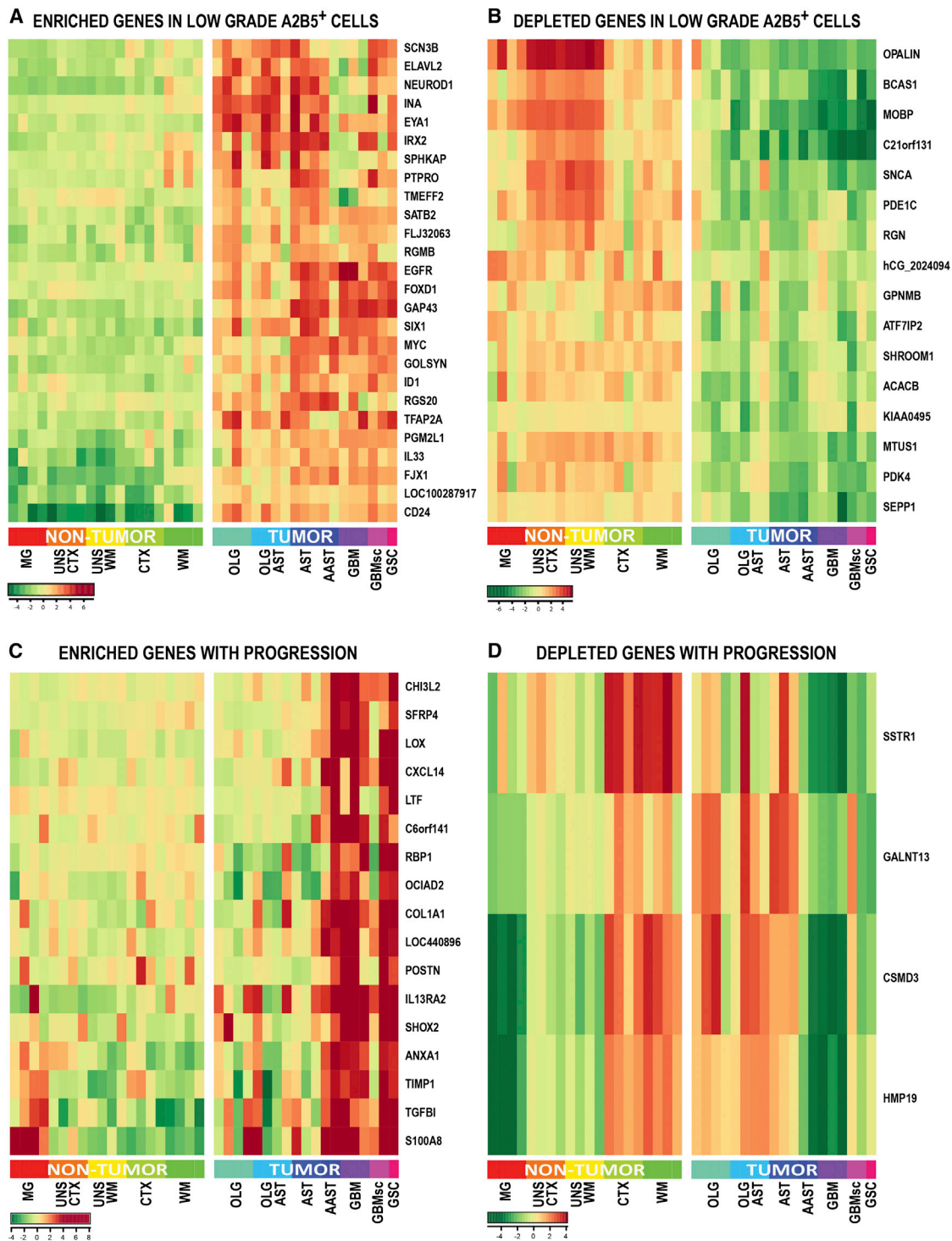
Figure 4. Expression Profiles of A2B5⁺ Cells during Early Tumorigenesis and Anaplastic Progression

(A and B) Heatmaps representing the top 26 upregulated (A; >10 FC, 1% FDR) and 16 downregulated genes (B; >5 FC, 1% FDR) from microarray analysis of LG-glioma-derived A2B5⁺ TPCs relative to normal A2B5⁺ GPCs isolated from either adult WM or cortex (CTX), or compared to CD11b microglial cells (MG).

(C and D) Heatmaps representing the top upregulated (C) and downregulated genes (D; >10 FC, 1% FDR) from microarray analysis of A2B5⁺ cells isolated from HG (WHO III-IV) tumors relative to their LG (WHO II) counterparts.

See also Table S9.
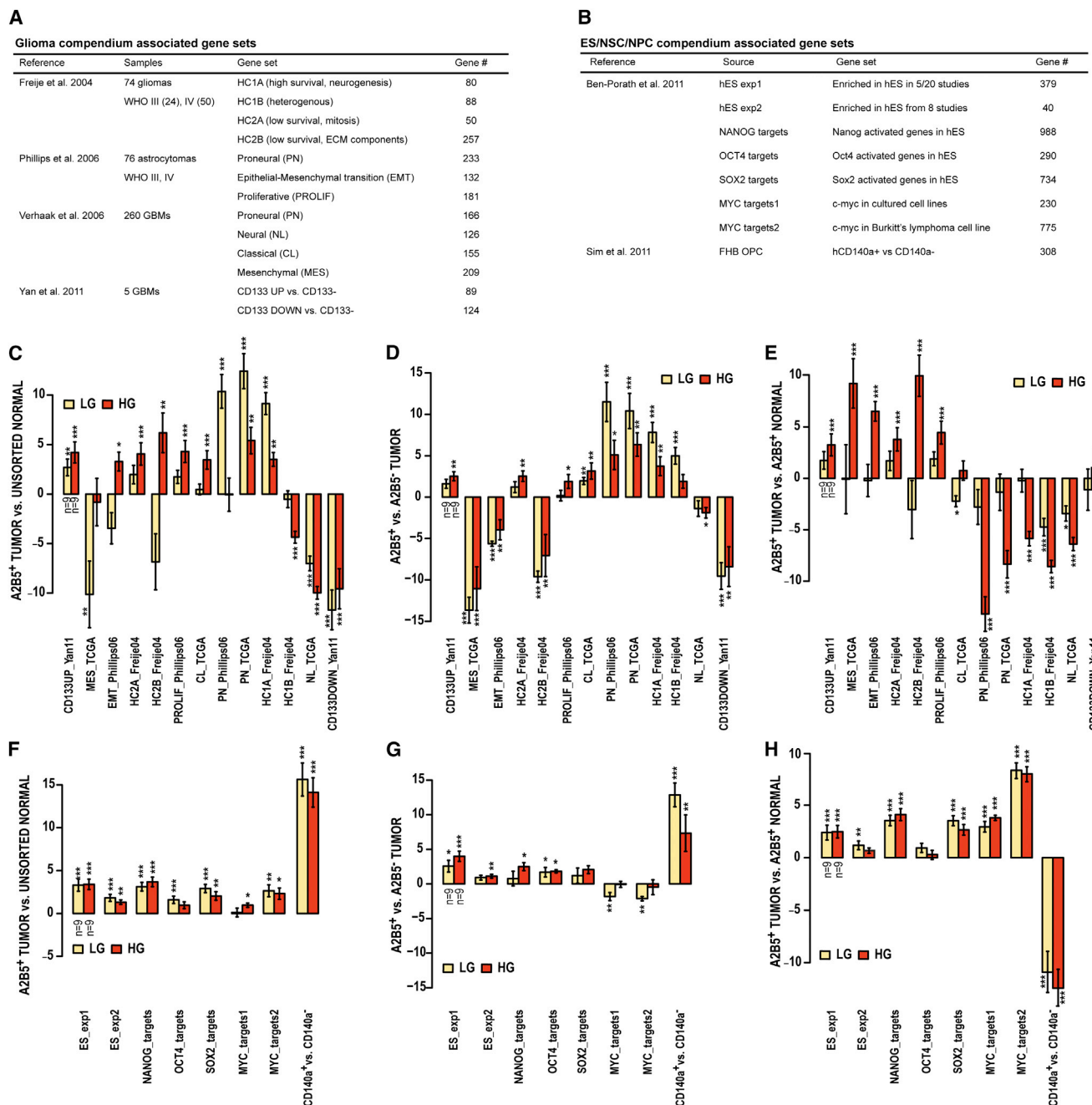
Figure 5. Molecular Homologies among A2B5^{+} TPCs, CD133^{+} TPCs, Gliomas, hESCs, and Normal GPCs

(A–H) Enrichment patterns of the A2B5^{+} glioma expression signature across previously established human glioma expression profiles, CD133^{+} TPCs, hESCs, and fetal human brain CD140a^{+} GPCs using parametric GSEA (PGSEA).

(A) List of gene sets associated with molecular subclasses of human gliomas and CD133-defined TPCs.

(B) Gene sets associated with hESCs, pluripotentiality-associated transcripts, and CD140a^{+} GPCs.

(C–H) PGSEA analysis of neoplastic A2B5^{+} cells compared with normal unsorted cells (C and F), neoplastic A2B5^{−} cells (D and G), and normal A2B5^{+} cells (E and H). To identify significant enrichment/depletion, a linear model approach was used and p values for each comparison were corrected for multiple testing using the FDR (q values). Significance indicated as follows: $*q < 0.05$, $**q < 0.01$, $***q < 0.001$. Data are expressed as average ± SEM.

See also Figures S7, S8, and S9.

epithelial cells. In addition, induced Six1 overexpression promotes the proliferation and metastatic dissemination of breast cancer cells and potentiates TGF-β signaling while inducing an EMT (Micalizzi et al., 2009). Extending these data, we found that SIX1 silencing inhibits the growth, proliferation, and survival of A2B5[+] TPCs in vitro and their tumorigenicity in vivo. The likely
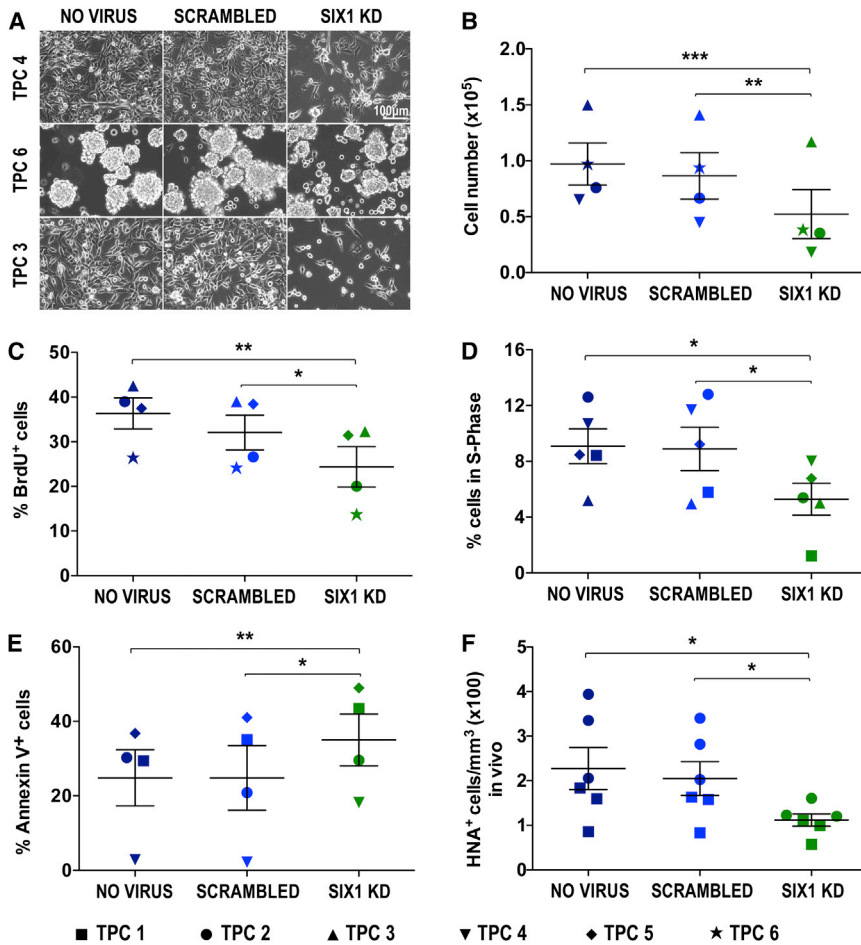
A NO VIRUS SCRAMBLED SIX1 KD

TPC 4 | TPC 6 | TPC 3

100μm

B

Cell number (x10^5)

***
**

NO VIRUS   SCRAMBLED   SIX1 KD

C

% BrdU$^+$ cells

**
*

NO VIRUS   SCRAMBLED   SIX1 KD

D

% cells in S-Phase

*
*

NO VIRUS   SCRAMBLED   SIX1 KD

E

% Annexin V$^+$ cells

**
*

NO VIRUS   SCRAMBLED   SIX1 KD

F

HNA$^+$ cells/mm^3 (x100) in vivo

*
*

NO VIRUS   SCRAMBLED   SIX1 KD

■ TPC 1   ● TPC 2   ▲ TPC 3   ▼ TPC 4   ◆ TPC 5   ★ TPC 6

Figure 6. SIX1 KD Impairs the Expansion and Survival of A2B5$^+$ TPCs In Vitro and In Vivo

(A–F) Effects of SIX1 KD on the in vitro growth (A and B), proliferation (C and D), and survival (E), as well as the in vivo tumorigenicity (F) of A2B5$^+$ TPCs at 6 days and 6 weeks, respectively, after transduction with either SIX1-KD lentivirus, scrambled shRNAi lentivirus, or nontransduced control. Six different glioma-derived tumor progenitor lines (TPC1-6) were used for this study, each specified by the symbols noted at the bottom of the figure.

(A and B) Representative photomicrographs (A) and graph (B) illustrating glioma cell numbers after transduction of TPC glioma lines by SIX1 KD or control vectors.

(C and D) Graphs illustrating the percentage of BrdU immunolabeling (C) and EdU incorporation (D) as a function of SIX1 KD.

(E and F) Effect of SIX KD on both apoptotic cell death as determined by flow cytometric analysis of Annexin V (E) and the number (F) of hNA$^+$ cells following transplantation of two distinct lines of glioma-derived A2B5$^+$ TPCs, each transduced with either SIX KD or control shRNAi. For each graph (B–F), horizontal lines indicate the mean value ± SEM; p values were calculated using one-way ANOVA with repeated measures followed by Tukey post hoc comparisons with *p < 0.05, **p < 0.01, and ***p < 0.001.

See also Figure S10.

importance of SIX1 overexpression in A2B5$^+$ glioma TPCs was emphasized by the simultaneous overexpression of EYA1, a principal coactivator of SIX1, at every stage of gliomagenesis, and the subsequent downregulation of its repressor, DACH2, during anaplastic progression (Christensen et al., 2008). Together, these data suggest that the SIX-EYA-DACH transcriptional complex plays a significant, hitherto unrecognized role in glial tumorigenesis.

In this study, we focused on A2B5$^+$ TPCs because A2B5 expression characterized a discrete population of progenitors that could be identified in normal brain, and serially tracked throughout disease progression. However, A2B5-defined TPCs were by no means the sole tumor-initiating cells. A2B5-depleted populations, particularly those derived from GBM, proved tumorigenic as well. Rather, the A2B5 pool appeared to identify an especially early-appearing and virulent phenotype. In matched comparisons, the A2B5$^+$ cells propagated new tumors at lower cell doses than did A2B5-depleted cells, and typically exhibited more rapid clonogenic expansion than did A2B5$^-$ cells derived from the same tumors. Together, these data suggest that multiple distinct tumor-initiating phenotypes, perhaps lineally related but nonetheless antigenically distinct, may coexist in GBM. The A2B5-defined phenotype is notable for appearing in the early stages of gliomagenesis and persisting during all

identified stages of tumor progression. Its selective expression of EMT genes with anaplastic progression suggests its role in tumor virulence, supported by the dominance of the A2B5 phenotype in sustained culture. Indeed, the dominance of this cell type in vitro portends both its aggressiveness and chemoresistance in vivo, since A2B5$^+$ glioma cells are preferentially resistant to the nitrosourea CCNU (Balik et al., 2009), one of the few approved chemotherapeutics for glioma.

More broadly, the A2B5-defined phenotype appears to comprise only one of several antigenically distinct glioma-propagating tumor progenitors each of which is independently capable of initiating tumor in a naive host. In this regard, it joins CD133 (Singh et al., 2004), CD15/SSEA1 (Son et al., 2009), and integrin-α6 (Lathia et al., 2010) as one of a number of only partially overlapping tumor-initiating phenotypes that together contribute to much of the virulence of malignant gliomas. Furthermore, the A2B5 phenotype itself may be heterogeneous, so it remains to be seen whether the A2B5-defined tumor signatures established in our study reflect the dysregulation of specific genes by all A2B5$^+$ TPCs, or instead reflect a specific subpopulation thereof. Given the diversity of tumor-initiating phenotypes within malignant glioma, our challenge is to identify and characterize the smallest possible set of nonoverlapping phenotypes that includes all cells capable of initiating tumors independently, and to then eliminate each phenotype separately, whether serially or concurrently, as a strategy for rational, phenotype-selective, and pathway-targeted tumor elimination.

EXPERIMENTAL PROCEDURES

Tissue Samples
Tumor samples were graded in accord with WHO guidelines as derived from oligodendroglioma, OLG (LG n = 4; anaplastic n = 4); astrocytoma, AST (diffuse n = 3; anaplastic n = 3); mixed oligoastrocytoma (LG n = 4; anaplastic n = 2); GBM (n = 16); or ganglioglioma (n = 1). Normal epileptic tissue resections obtained from 54 patients were used as controls. Among these, a set of matched gray-matter- and WM-derived A2B5-sorted GPCs were isolated from four patients (30–46 years old). All samples were obtained from patients who consented to tissue use, under protocols approved by the institutional review boards of both the University of Rochester and Johns Hopkins University.

Cell Preparation and Isolation
Tissues were dissociated using papain, cultured in cell suspension plates, in serum-free media (SFM) defined as Dulbecco's modified Eagle's medium (DMEM)/F12 media supplemented with N1, 20 ng/ml basic FGF (bFGF), EGF, and PDGF-AA. Tumor-derived GPCs were then isolated by tissue dissociation, followed by A2B5-based cell sorting (both MACS and FACS), using previously described protocols (Nunes et al., 2003).

Orthotopic Transplantation and Analysis
To assess in vivo tumorigenicity, adult immunodeficient mice were injected with TPCs of the sorted phenotypes noted, and killed at various time points thereafter. All transplantation procedures were reviewed and approved by the Rochester University Committee on Animal Resources. At the time of sacrifice, xenografted brains were cut and donor cells identified by immunolabeling for human nuclear antigen, human glial fibrillary acidic protein (GFAP), or human nestin, as well as Ki67, survivin, and P53. The antibodies used are listed in Table S10.

Differential Gene-Expression and Pathway Analysis
RNA isolated from A2B5-selected cells was labeled and hybridized to Affymetrix U133+2 arrays. All analyses were performed in R/Bioconductor. Microarray data were preprocessed using robust multichip analysis (RMA) and informative probe sets were subsequently determined using factor analysis for robust microarray summarization (FARMS). PCA and hierarchical clustering were performed on normalized data. Differential gene-expression analysis was performed using a linear model approach, employing an empirical Bayesian method for calculation of statistical significance (Bioconductor, limma package). A 3-fold change threshold with significance at 1% FDR was generally applied to define differential expression. Pathway analyses were performed using IPA, as well as several open-source systems.

Clonogenicity, Multipotency, Cell Proliferation, and Cell Death Assays
Clonogenicity was assessed 14 days after dissociation of gliomaspheres into single cells and distributed to 96-well plates at 5–100 cells/well with 0.2 ml/well of SFM. Multipotency was examined on individual spheres cultured in DMEM/F12/N1 with 1% fetal bovine serum (FBS) for up to 12 days. The cells were then fixed and immunostained for GFAP, Olig2, CNP, βIII-tubulin, or MAP-2AB, followed by Alexa-Fluor conjugated secondary antibodies. Cell-proliferation and cell-cycle analyses were performed using BrdU (30 μM) and EdU (10 μM) administration followed by immunocytochemical analysis and Click-it-based Edu flow cytometry analysis (Invitrogen), respectively, according to the manufacturer's instructions. Cell apoptosis and cell death were assessed by flow cytometry analysis of Annexin V (BD) and DAPI, respectively.

Generation, Validation, and Assessment of Six1 KD Lentivirus
A set of five lentiviral shRNAi vectors with distinct target sequences was purchased from Open Biosystems. SIX1 silencing constructs were validated by transfection of multiple glioma cell lines, with subsequent qPCR and western immunoblot detection of SIX1 mRNA and protein expression. Viral production, cell transduction, validation of KD, and assessment of effects thereof on glioma cell proliferation and death are all described in the Extended Experimental Procedures.

Statistical Analysis
Statistical analysis for all experiments including more than two groups was performed using a one-way or two-way ANOVA followed by post hoc comparisons using the Tukey multiple-comparisons test. For experiments with two groups, Student's t test was used.

ACCESSION NUMBERS

The microarray data described herein are available at the NCBI Gene Expression Omnibus under accession number GSE29796.

SUPPLEMENTAL INFORMATION

Supplemental Information includes Extended Experimental Procedures, ten figures, and ten tables and can be found with this article online at http://dx.doi.org/10.1016/j.celrep.2013.04.035.

LICENSING INFORMATION

This is an open-access article distributed under the terms of the Creative Commons Attribution-NonCommercial-No Derivative Works License, which permits non-commercial use, distribution, and reproduction in any medium, provided the original author and source are credited.

REFERENCES

Alcantara Llaguno, S., Chen, J., Kwon, C.H., Jackson, E.L., Li, Y., Burns, D.K., Alvarez-Buylla, A., and Parada, L.F. (2009). Malignant astrocytomas originate from neural stem/progenitor cells in a somatic tumor suppressor mouse model. Cancer Cell 15, 45–56.

Assanah, M., Lochhead, R., Ogden, A., Bruce, J., Goldman, J., and Canoll, P. (2006). Glial progenitors in adult white matter are driven to form malignant gliomas by platelet-derived growth factor-expressing retroviruses. J. Neurosci. 26, 6781–6790.

Balik, V., Mirossay, P., Bohus, P., Sulla, I., Mirossay, L., and Sarissky, M. (2009). Flow cytometry analysis of neural differentiation markers expression in human glioblastomas may predict their response to chemotherapy. Cell. Mol. Neurobiol. 29, 845–858.

Bao, S., Wu, Q., McLendon, R.E., Hao, Y., Shi, Q., Hjelmeland, A.B., Dewhirst, M.W., Bigner, D.D., and Rich, J.N. (2006). Glioma stem cells promote radioresistance by preferential activation of the DNA damage response. Nature 444, 756–760.

Baumann, P., Cremers, N., Kroese, F., Orend, G., Chiquet-Ehrismann, R., Uede, T., Yagita, H., and Sleeman, J.P. (2005). CD24 expression causes the acquisition of multiple cellular properties associated with tumor growth and metastasis. Cancer Res. 65, 10783–10793.

Christensen, K.L., Patrick, A.N., McCoy, E.L., and Ford, H.L. (2008). The six family of homeobox genes in development and cancer. Adv. Cancer Res. *101*, 93–126.

Deng, J., Gao, G., Wang, L., Wang, T., Yu, J., and Zhao, Z. (2012). CD24 expression as a marker for predicting clinical outcome in human gliomas. J. Biomed. Biotechnol. *2012*, 517172.

Di Benedetto, M., Bièche, I., Deshayes, F., Vacher, S., Nouet, S., Collura, V., Seitz, I., Louis, S., Pineau, P., Amsellem-Ouazana, D., et al. (2006). Structural organization and expression of human MTUS1, a candidate 8p22 tumor suppressor gene encoding a family of angiotensin II AT2 receptor-interacting proteins, ATIP. Gene *380*, 127–136.

Earl, J., Yan, L., Vitone, L.J., Risk, J., Kemp, S.J., McFaul, C., Neoptolemos, J.P., Greenhalf, W., Kress, R., Sina-Frey, M., et al.; European Registry of Hereditary Pancreatitis and Familial Pancreatic Cancer; German National Case Collection for Familial Pancreatic Cancer. (2006). Evaluation of the 4q32-34 locus in European familial pancreatic cancer. Cancer Epidemiol. Biomarkers Prev. *15*, 1948–1955.

Feigenson, K., Reid, M., See, J., Crenshaw, E.B., 3rd, and Grinspan, J.B. (2009). Wnt signaling is sufficient to perturb oligodendrocyte maturation. Mol. Cell. Neurosci. *42*, 255–265.

Freije, W.A., Castro-Vargas, F.E., Fang, Z., Horvath, S., Cloughesy, T., Liau, L.M., Mischel, P.S., and Nelson, S.F. (2004). Gene expression profiling of gliomas strongly predicts survival. Cancer Res. *64*, 6503–6510.

Galli, R., Binda, E., Orfanelli, U., Cipelletti, B., Gritti, A., De Vitis, S., Fiocco, R., Foroni, C., Dimeco, F., and Vescovi, A. (2004). Isolation and characterization of tumorigenic, stem-like neural precursors from human glioblastoma. Cancer Res. *64*, 7011–7021.

Hedge, T.A., and Mason, I. (2008). Expression of Shisa2, a modulator of both Wnt and Fgf signaling, in the chick embryo. Int. J. Dev. Biol. *52*, 81–85.

Hemmati, H.D., Nakano, I., Lazareff, J.A., Masterman-Smith, M., Geschwind, D.H., Bronner-Fraser, M., and Kornblum, H.I. (2003). Cancerous stem cells can arise from pediatric brain tumors. Proc. Natl. Acad. Sci. USA *100*, 15178–15183.

Ignatova, T.N., Kukekov, V.G., Laywell, E.D., Suslov, O.N., Vrionis, F.D., and Steindler, D.A. (2002). Human cortical glial tumors contain neural stem-like cells expressing astroglial and neuronal markers in vitro. Glia *39*, 193–206.

Ikushima, H., Todo, T., Ino, Y., Takahashi, M., Miyazawa, K., and Miyazono, K. (2009). Autocrine TGF-beta signaling maintains tumorigenicity of glioma-initiating cells through Sry-related HMG-box factors. Cell Stem Cell *5*, 504–514.

Jackson, E.L., Garcia-Verdugo, J.M., Gil-Perotin, S., Roy, M., Quinones-Hinojosa, A., VandenBerg, S., and Alvarez-Buylla, A. (2006). PDGFR alpha-positive B cells are neural stem cells in the adult SVZ that form glioma-like growths in response to increased PDGF signaling. Neuron *51*, 187–199.

Langford, L.A., Piatyszek, M.A., Xu, R., Schold, S.C., Jr., and Shay, J.W. (1995). Telomerase activity in human brain tumours. Lancet *346*, 1267–1268.

Lathia, J.D., Gallagher, J., Heddleston, J.M., Wang, J., Eyler, C.E., Macswords, J., Wu, Q., Vasanji, A., McLendon, R.E., Hjelmeland, A.B., and Rich, J.N. (2010). Integrin alpha 6 regulates glioblastoma stem cells. Cell Stem Cell *6*, 421–432.

Ligon, K.L., Huillard, E., Mehta, S., Kesari, S., Liu, H., Alberta, J.A., Bachoo, R.M., Kane, M., Louis, D.N., Depinho, R.A., et al. (2007). Olig2-regulated lineage-restricted pathway controls replication competence in neural stem cells and malignant glioma. Neuron *53*, 503–517.

Lindberg, N., Kastemar, M., Olofsson, T., Smits, A., and Uhrbom, L. (2009). Oligodendrocyte progenitor cells can act as cell of origin for experimental glioma. Oncogene *28*, 2266–2275.

Liu, C., Sage, J.C., Miller, M.R., Verhaak, R.G., Hippenmeyer, S., Vogel, H., Foreman, O., Bronson, R.T., Nishiyama, A., Luo, L., and Zong, H. (2011). Mosaic analysis with double markers reveals tumor cell of origin in glioma. Cell *146*, 209–221.

Micalizzi, D.S., Christensen, K.L., Jedlicka, P., Coletta, R.D., Barón, A.E., Harrell, J.C., Horwitz, K.B., Billheimer, D., Heichman, K.A., Welm, A.L., et al. (2009). The Six1 homeoprotein induces human mammary carcinoma cells to

undergo epithelial-mesenchymal transition and metastasis in mice through increasing TGF-beta signaling. J. Clin. Invest. *119*, 2678–2690.

Midorikawa, Y., Tsutsumi, S., Taniguchi, H., Ishii, M., Kobune, Y., Kodama, T., Makuuchi, M., and Aburatani, H. (2002). Identification of genes associated with dedifferentiation of hepatocellular carcinoma with expression profiling analysis. Jpn. J. Cancer Res. *93*, 636–643.

Mishra, L., Derynck, R., and Mishra, B. (2005). Transforming growth factor-beta signaling in stem cells and cancer. Science *310*, 68–71.

Nishide, K., Nakatani, Y., Kiyonari, H., and Kondo, T. (2009). Glioblastoma formation from cell population depleted of Prominin1-expressing cells. PLoS ONE *4*, e6869.

Nishiyama, A., Komitova, M., Suzuki, R., and Zhu, X. (2009). Polydendrocytes (NG2 cells): multifunctional cells with lineage plasticity. Nat. Rev. Neurosci. *10*, 9–22.

Nunes, M.C., Roy, N.S., Keyoung, H.M., Goodman, R.R., McKhann, G., 2nd, Jiang, L., Kang, J., Nedergaard, M., and Goldman, S.A. (2003). Identification and isolation of multipotential neural progenitor cells from the subcortical white matter of the adult human brain. Nat. Med. *9*, 439–447.

Ogden, A.T., Waziri, A.E., Lochhead, R.A., Fusco, D., Lopez, K., Ellis, J.A., Kang, J., Assanah, M., McKhann, G.M., Sisti, M.B., et al. (2008). Identification of A2B5+CD133- tumor-initiating cells in adult human gliomas. Neurosurgery *62*, 505–514, discussion 514–505.

Pandey, R.N., Rani, R., Yeo, E.J., Spencer, M., Hu, S., Lang, R.A., and Hegde, R.S. (2010). The Eyes Absent phosphatase-transactivator proteins promote proliferation, transformation, migration, and invasion of tumor cells. Oncogene *29*, 3715–3722.

Patani, N., Jiang, W., Mansel, R., Newbold, R., and Mokbel, K. (2009). The mRNA expression of SATB1 and SATB2 in human breast cancer. Cancer Cell Int. *9*, 18.

Patel, Y.C. (1999). Somatostatin and its receptor family. Front. Neuroendocrinol. *20*, 157–198.

Persson, A.I., Petritsch, C., Swartling, F.J., Itsara, M., Sim, F.J., Auvergne, R., Goldenberg, D.D., Vandenberg, S.R., Nguyen, K.N., Yakovenko, S., et al. (2010). Non-stem cell origin for oligodendroglioma. Cancer Cell *18*, 669–682.

Phillips, H.S., Kharbanda, S., Chen, R., Forrest, W.F., Soriano, R.H., Wu, T.D., Misra, A., Nigro, J.M., Colman, H., Soroceanu, L., et al. (2006). Molecular subclasses of high-grade glioma predict prognosis, delineate a pattern of disease progression, and resemble stages in neurogenesis. Cancer Cell *9*, 157–173.

Pincus, D.W., Keyoung, H.M., Harrison-Restelli, C., Goodman, R.R., Fraser, R.A., Edgar, M., Sakakibara, S., Okano, H., Nedergaard, M., and Goldman, S.A. (1998). Fibroblast growth factor-2/brain-derived neurotrophic factor-associated maturation of new neurons generated from adult human subependymal cells. Ann. Neurol. *43*, 576–585.

Pouly, S., Becher, B., Blain, M., and Antel, J.P. (1999). Expression of a homologue of rat NG2 on human microglia. Glia *27*, 259–268.

Pulvirenti, T., Van Der Heijden, M., Droms, L.A., Huse, J.T., Tabar, V., and Hall, A. (2011). Dishevelled 2 signaling promotes self-renewal and tumorigenicity in human gliomas. Cancer Res. *71*, 7280–7290.

Sanai, N., Tramontin, A.D., Quiñones-Hinojosa, A., Barbaro, N.M., Gupta, N., Kunwar, S., Lawton, M.T., McDermott, M.W., Parsa, A.T., Manuel-García Verdugo, J., et al. (2004). Unique astrocyte ribbon in adult human brain contains neural stem cells but lacks chain migration. Nature *427*, 740–744.

Senner, V., Sturm, A., Baur, I., Schrell, U.H., Distel, L., and Paulus, W. (1999). CD24 promotes invasion of glioma cells in vivo. J. Neuropathol. Exp. Neurol. *58*, 795–802.

Shih, A.H., and Holland, E.C. (2006). Platelet-derived growth factor (PDGF) and glial tumorigenesis. Cancer Lett. *232*, 139–147.

Sim, F.J., Lang, J.K., Waldau, B., Roy, N.S., Schwartz, T.E., Pilcher, W.H., Chandross, K.J., Natesan, S., Merrill, J.E., and Goldman, S.A. (2006). Complementary patterns of gene expression by human oligodendrocyte progenitors

and their environment predict determinants of progenitor maintenance and differentiation. Ann. Neurol. *59*, 763–779.

Sim, F.J., McClain, C.R., Schanz, S.J., Protack, T.L., Windrem, M.S., and Goldman, S.A. (2011). CD140a identifies a population of highly myelinogenic, migration-competent and efficiently engrafting human oligodendrocyte progenitor cells. Nat. Biotechnol. *29*, 934–941.

Singh, S.K., Hawkins, C., Clarke, I.D., Squire, J.A., Bayani, J., Hide, T., Henkelman, R.M., Cusimano, M.D., and Dirks, P.B. (2004). Identification of human brain tumour initiating cells. Nature *432*, 396–401.

Son, M.J., Woolard, K., Nam, D.H., Lee, J., and Fine, H.A. (2009). SSEA-1 is an enrichment marker for tumor-initiating cells in human glioblastoma. Cell Stem Cell *4*, 440–452.

Stupp, R., Mason, W.P., van den Bent, M.J., Weller, M., Fisher, B., Taphoorn, M.J., Belanger, K., Brandes, A.A., Marosi, C., Bogdahn, U., et al.; European Organisation for Research and Treatment of Cancer Brain Tumor and Radio-therapy Groups; National Cancer Institute of Canada Clinical Trials Group. (2005). Radiotherapy plus concomitant and adjuvant temozolomide for glioblastoma. N. Engl. J. Med. *352*, 987–996.

Tchoghandjian, A., Baeza, N., Colin, C., Cayre, M., Metellus, P., Beclin, C., Ouafik, L., and Figarella-Branger, D. (2010). A2B5 cells from human glioblastoma have cancer stem cell properties. Brain Pathol. *20*, 211–221.

Verhaak, R.G., Hoadley, K.A., Purdom, E., Wang, V., Qi, Y., Wilkerson, M.D., Miller, C.R., Ding, L., Golub, T., Mesirov, J.P., et al.; Cancer Genome Atlas Research Network. (2010). Integrated genomic analysis identifies clinically relevant subtypes of glioblastoma characterized by abnormalities in PDGFRA, IDH1, EGFR, and NF1. Cancer Cell *17*, 98–110.

Wang, J., Wang, H., Li, Z., Wu, Q., Lathia, J.D., McLendon, R.E., Hjelmeland, A.B., and Rich, J.N. (2008). c-Myc is required for maintenance of glioma cancer stem cells. PLoS ONE *3*, e3769.